Journal of Computer Science and Artificial Intelligence
ISSN: 3078-8242 (Print), ISSN: 3078-2309 (Online) | Vol. 2, No. 3, 2025

Feature Extraction and Analysis of Multilayer Higher-Order Brain Functional Networks in Patients with Schizophrenia

Jianghao Zhao, Guimei Yin *

School of Computer Science and Technology, Taiyuan Normal University, Jinzhong 030619, China

Abstract: Objectives: A schizophrenia patient model based on Persistent homology and multilayer brain networks combines full-frequency band information to mine and categorize key brain regions, providing a decision-making basis for patient treatment. Methods: Using the information of 198 subjects from Huilongguan Hospital in Beijing who met the requirements of this study, the network features based on the constructed multilayer brain network were mined by Persistent homophony and traditional methods of mining multi-frequency band information of subjects, and finally analyzed by using a deep learning model. Results: After the lesion, the brain area changes were mainly in the frontal central cortex and left parietal lobe, leading to the alteration of the patient's perceptual and cognitive abilities, and the classification training using a deep learning model resulted in a classification accuracy of 92.3%. Conclusion: By constructing a multilayer brain network model and using a persistent homology approach, cross-frequency band information can be effectively utilized, and higher-order information can be exploited to improve disease diagnosis.

Keywords: Multilayer network, Persistent homology, EEG, Schizophrenia.

1. Introduction

Schizophrenia is a common chronic disabling mental disorder, although its neurological basis is unclear. Relevant studies have shown that schizophrenia is a complex mental disorder typically characterized by abnormalities in whole-brain connectivity, and its underlying neuropathology is related to abnormal coordination of the patient's functioning in multiple brain regions [1, 2].

Brain activity is frequency-specific and different physiological activities produce frequency-specific signals. Recent studies have found that brain network differences in schizophrenia occur at different frequencies [3, 4]. Researchers have also found that people with schizophrenia exhibit broad band-specific differences in low-frequency amplitude and regional coherence [5]. However, previous studies have shown that cross-frequency coupling is used in the deployment of spatial attention during visuomotor tasks whereas the study of intra- or inter-band interactions at specific frequencies plays an important role in the study of schizophrenia [6, 7]. Therefore, different frequency bands cannot simply be considered as a single entity. Neglecting the interactions between frequency bands may lead to the loss of some important information [8].

It has been shown that differences in the function of some of the same nodes appear under single-layer and multilayer networks, while multilayer networks can integrate both intra- and inter-layer interdependencies [9]. Many scholars have already used multilayer networks to capture network global information, such as in adolescent myoclonic epilepsy by building multilayer brain networks to study the modular changes in brain network function and the differences between healthy subjects after lesions of specific functional networks [10]. Changes produced by building multilayer brain networks for normal subjects versus headache patients after lesions of specific functional networks [11]. For patients with schizophrenia, it has been shown that patients with schizophrenia have disorganized brain network topological features compared to healthy subjects [12]. This suggests that patients have dysfunctional brain functional network organization. Therefore, we used multilayer networks for the study of functional networks in schizophrenia. Here, we explored the dynamic functional characteristics of the whole brain of schizophrenic patients from a multifrequency perspective. First, we constructed a multilayer network model; then, we introduced the sustained homology theory to be applied in the multilayer network, and assessed the integration and separation characteristics of the multilayer frequency brain network in schizophrenia patients. In addition, we explored the significant changes in brain regions when schizophrenia patients had lesions to further assess the correlation between the multilayer network characteristics and patients' clinical symptoms, and finally, we used the deep learning model to discriminate the classification of schizophrenia patients.

2. Basic Principles

2.1. Simplex and Simplex Complex

A simplex is a geometric structure commonly used in topological data analysis, while a simplex complex is a combination of simplexes with the property that it can approximate any complex shape and is easy to compute. Due to the lack of direct methods to extract topological information from data points, simplexes are often constructed as topological approximations of the underlying shapes of sampled points in topological data analysis. Here the simple complex shape can be viewed as a high-dimensional extension of a graph [13, 14].

The essence of a simplex is the generalization of a triangle to each dimension, an abstract simplex is any finite set of vertices, a simplex I= $\{a, b\}$ is one-dimensional while a simplex J= $\{a, b, c\}$ is two-dimensional, etc. k-dimensional simplexes are illustrated in Fig. 1, where vertices (k=0) are zero-dimensional simplexes, edges (k=1) are one-dimensional simplexes, and triangles (k=2) are two-dimensional simplexes, tetrahedron (k=3) is a three-dimensional simplex [15].

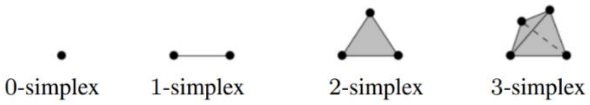

Figure 1. k-dimensional simplex

The set of simplexes is a simplex complex, and for each simplex K, the following two conditions are satisfied (1) any face of any simplex in K still belongs to K, and (2) the intersection of any two simplexes in K is either the empty set or one of the faces shared by both. Figure 2 shows a simplex complex containing two two-dimensional simplexes (triangles) connected along one edge and another two-dimensional simplex connected by a one-dimensional simplex (line segment). Since the highest dimensional simplex contained in this simplex is two-dimensional, it is called a two-dimensional simplex.

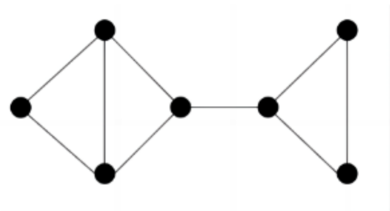

Figure 2. two-dimensional simple complex

2.2. Constant Homology

Clustering coefficients in brain networks are important metrics used to statistically compute the processing power of the local information of nodes, and in this paper, we use persistent homology to capture continuously changing topological information in the metric space. First, Vietoris-Rips (VR) complex shapes of different dimensions are constructed according to a specified threshold ε (when ε is larger than the metric between nodes in the network, a line is formed between two points), and the process is illustrated in Fig. 3, which results in the persistent topological feature in different dimensions, i.e., 0-dimensional, 1-dimensional, and 2-dimensional Betti numbers, etc. The feature is usually visualized with Persistence Diagram (PD) or barcode [16, 17].

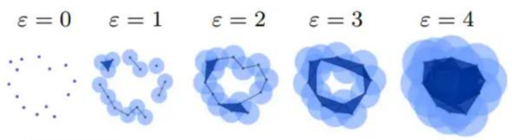

Figure 3. Examples of simplex complexes of different dimensions

The existence of multilayer networks greatly enriches the existence of complex shapes in the network, and the edges of simple complex shapes may all be distributed in a certain layer, or they may be distributed in different layers respectively to exchange the point cloud coordinates of isomorphic neighboring layers to form the extraction of simple complex shapes in multilayer networks.

2.3. Graphical Convolutional Neural Network

GCN is a graph neural network model for processing graph-structured data. GCN performs information propagation and feature learning on graph data through convolutional operations, which enables each node to aggregate information from its neighboring nodes to achieve tasks such as feature learning and node classification on graph data [18, 19].

The core idea of GCN is based on graph convolution operation. For a graph containing N nodes, GCN introduces a learnable parameter matrix to linearly transform the features of the nodes [20]. By weighted summation of the features of neighboring nodes, each node gets an updated feature representation. The graph convolution operation of GCN can be expressed as the following equation:

$$H^{(l+1)} = \sigma\left(\tilde{D}^{-\frac{1}{2}}\tilde{A}\tilde{D}^{-\frac{1}{2}}H^{(l)}W^{(l)}\right) \tag{1}$$

Where $\tilde{A}$=A+I, I is the unit matrix, $\tilde{D}$ is the degree matrix (degree matrix) of $\tilde{A}$, H is the features of each layer, and σ is the nonlinear activation function.

The graph convolution operation through multiple layers enables each node to aggregate information about a wider range of neighboring nodes, thus enabling a hierarchical representation of node features and the learning of complex relationships, with the layer feature propagation formula of:

$$f\left(H^{(l)}, A\right) = \sigma\left(\tilde{D}^{-\frac{1}{2}}\tilde{A}\tilde{D}^{-\frac{1}{2}}H^{(l)}W^{(l)}\right) \tag{2}$$

Ultimately, GCN can perform tasks such as node classification, link prediction, and graph representation learning with node feature vectors. However, GCN cannot specify different weights for different nodes in the neighborhood.

3. Experimentation

This paper proposes a method of multilayer network modeling and its analysis for schizophrenia patients, the overall process is divided into three parts of processing, first for the collection of EEG data and preprocessing, through the preprocessing data will be divided into five frequency bands, in the construction of multilayer network, within the layer based on the Pearson correlation coefficient to build a single-layer brain network, between the layers of the adjacent layers of the same nodes for inter-layer linking, and finally based on the multilayer network metrics to find significant brain regions and patient classification downstream tasks. The experimental flow of this study is shown in Figure 4.

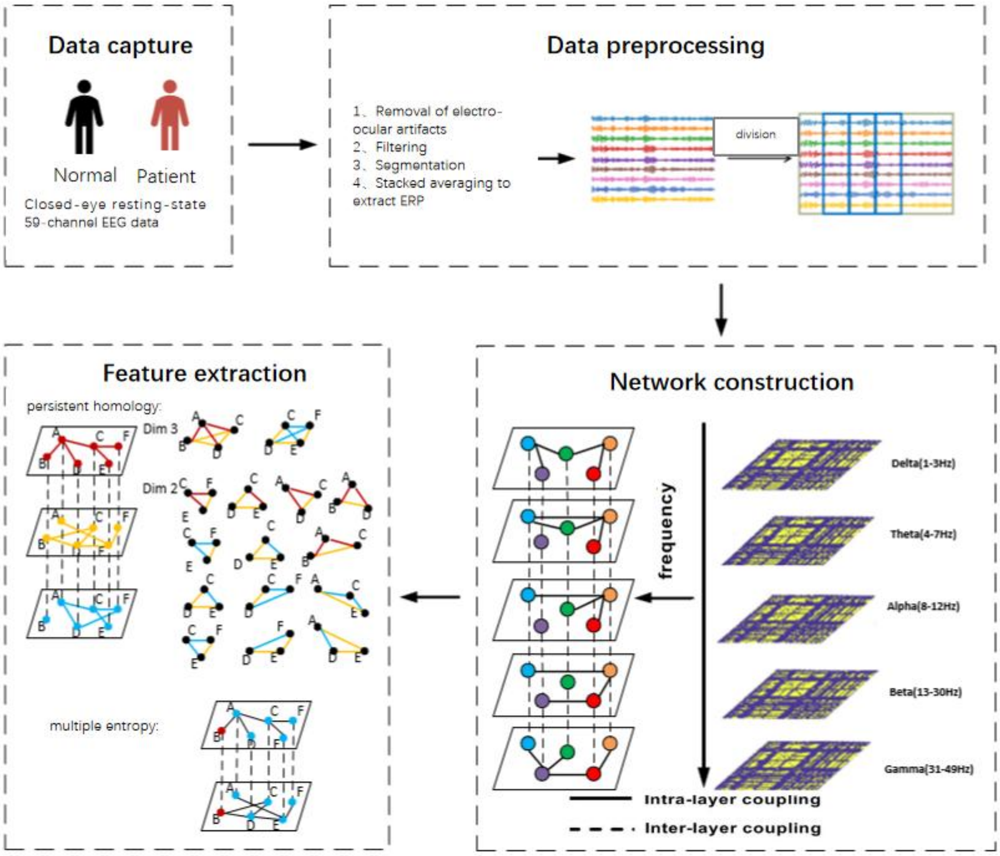

Figure 4. Experimental flow chart

3.1. Experimental Subject

The experiment used 59-channel EEG data collected under closed-eye resting state from 104 first-episode stemmatological patients and 94 healthy subjects in Huilongguan Hospital, Beijing, China. Matching was done by gender, age, and education level, and the demographics, PANNS scores, and other clinical data statistical information of the two groups of subjects are shown in Table 1.

3.2. Data Preprocessing

Experiments were performed using Python's MNE toolkit to preprocess the EEG signal data. The signal was filtered into five frequency bands, Delta (1-3 Hz), Theta (4-7 Hz), Alpha (8-12 Hz), Beta (13-30 Hz), and Gamma (31-49 Hz). The time length of each sample data was about 230 s. A sliding window (length=10 s TR=10 s) was utilized to intercept the data from 40 s-200 s to represent the topology of the brain. Repeated experiments were performed on all EEG signals through non-overlapping sliding windows.

Table 1. Table of demographic and clinical data statistics for subjects in both groups

Features	Schizophrenic patients (n = 104)	Health subjects (n= 94)	Statistical value
Average age (years)	30.49 (20-50)	30.50 (17-48)	F1,196< 1
Time of education (years)	14.15 (9-19)	14.73 (9-19)	F 1,196 = 2.697, p = 0.102
Gender (male/female)	52/52	50/44	χ12 = 0.201, p = 0.654
PANSS score	75.28 ± 11.10		
Positive score	21.77 ± 4.89		
Negative score	17.32 ± 5.84		

3.3. Single-Layer Network Construction

Each time window was taken as a sample, and the brain network was constructed and used as a graph structure by using the Pearson correlation value between time series as the functional connectivity value between brain regions, and 59 brain regions were extracted from the EEG data by relying on the operating guidelines of clinical EEG technology [3], which were set up as each node, and a 59 × 59 distance matrix was extracted, and the Pearson correlation value between time series was used as the functional connectivity value between brain regions. functional connectivity values between them. For each node, a 59×59 neighbor matrix was constructed by dynamically adjusting the threshold for binarization according to its PLV value with other nodes.

3.4. Multilayer Network Construction

For multilayer networks, there is a common representation: the block adjacency matrix. A multilayer network with layering can be represented as:

$$\boldsymbol{A} = \begin{bmatrix} A_1 & \cdots & H_{1f} \\ \vdots & \ddots & \vdots \\ H_{f1} & \cdots & A_f \end{bmatrix} \tag{3}$$

Where A_α is denoted as the symmetric square matrix of layer $\propto$, $1 \ll \propto \ll f$, and H_{kl} is the connection matrix between layer k and layer l, $1 \ll k, 1 \ll f$. Each layer has the same dimension as the neighbor matrix $(N * N)$. In this paper, a multilayer network based on EEG signal data is constructed by integrating five (Delta, Theta, Alpha, Beta, Gamma) frequency specific networks, in which each layer shares the same set of nodes (N=59), and the constructed single-layer brain network is used within the layers, and the same nodes are connected between the layers, disregarding different node connections in different frequency bands.

3.5. Multilayer Centrality Metric

The centrality property of multilayer networks was calculated. The importance of a region relative to the overall functional connectivity of the brain can be quantified by a centrality measure. The "degree" in a single-layer network is extended to a multi-layer network and is called "node overlap" [21]. However, in multilayer networks, there may exist node a and node b with the same degree of node overlap, but the degree of distribution in different layers is different, resulting in the two nodes have different roles in the network. Therefore, multilayer entropy (EMD) is proposed as an indicator to react to the distribution of nodes in different layers to judge the function of nodes in multilayer networks.

The higher the EMD value, the more uniformly the nodes are distributed in each layer, and the more role the nodes play in the layers. Therefore, in this paper we use the EMD value to denote the global processing power of the network. In multilayer networks, we define the multilayer entropy EMD formula as:

$$M_i = -\sum_{a=1}^{M} \frac{K_i^{[a]}}{O_i} \ln\left(\frac{K_i^{[a]}}{O_i}\right) \quad (4)$$

Where $\propto$ denotes a layer in a multilayer network, M is the number of layers, $k_i^{[\propto]}$ denotes the degree value of node i on layer $\propto$, and O_i denotes the overlap degree of node i. O_i is related to $k_i^{[\propto]}$ as follows:

$$O_i = \sum_{a=1}^{M} K_i^{[a]} \quad (5)$$

The multiple entropy of a multilayer network can be expressed as the average of the EMD of each node:

$$E = \frac{1}{N}\sum_{i=1}^{N} E_i \quad (6)$$

3.6. Feature Extraction

The experiment uses Pymnet library in Python for multilayer brain network construction with Giotto-TDA topology machine learning toolbox for VR complex shape extraction. Based on the Pearson correlation coefficient constructed for each frequency band of the single-layer brain network, extract its edge weight matrix in the conversion to point cloud coordinates, that is, for each layer of the brain network, to get the point cloud coordinates of its 59 nodes, the neighboring layer of the same node point cloud coordinates, point cloud coordinate exchange to achieve the cross-layer information interaction, and ultimately into the Giotto-TDA toolbox for the extraction of simplex complex shapes, to realize the cross-layer simplex complex shape Construction. Figure 5 shows the visualization of the brain network after the exchange of cross-layer point cloud coordinates, and the red node, i.e., the point cloud coordinates of the 20th brain region in the adjacent layer, is interacted with the visualization of the adjacent layer.

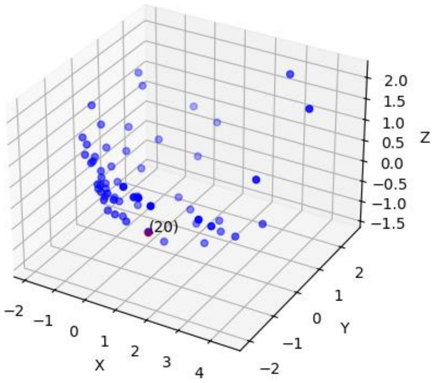

Figure 5. Cross-layer visualization of point cloud coordinates

Based on the constructed multilayer brain network, the multiple entropy of each node is calculated. For each extracted simplex complex, based on the circle ratio, the number of times each node participates in the simplex complex is calculated to derive the circle ratio value.

In the process of researching and designing high-dimensional topological features, since the persistence diagram PD obtained by VR filtering flow does not directly enter into machine learning algorithms for classification, based on the existing methods of topological data analysis, we convert the persistence diagram PD into persistence landscape diagram PL, Betti curve BC, and heat kernel diagram HK, which are able to observe the characteristics of the obtained persistence diagram PD from different dimensions. Compared to directly extracting features from complex EEG temporal data for classification, extracting topological features from the persistence map PD is highly interpretable and visualizable. In order to highly profile the three topological feature maps obtained, we summarize the PL, BC, and HK using matrix paradigms (1-paradigm vs. 2-paradigm), and obtain a matrix paradigm in each dimension of the VR complex shape to obtain the feature values that can be used for machine learning classification, in the process shown in Fig. 6. The feature formulae are then described in terms of reasoning, and feature representations as shown in Table 2 for the topological features of the experimental field and the corresponding parameter selection and realization are investigated and proved to be effective.

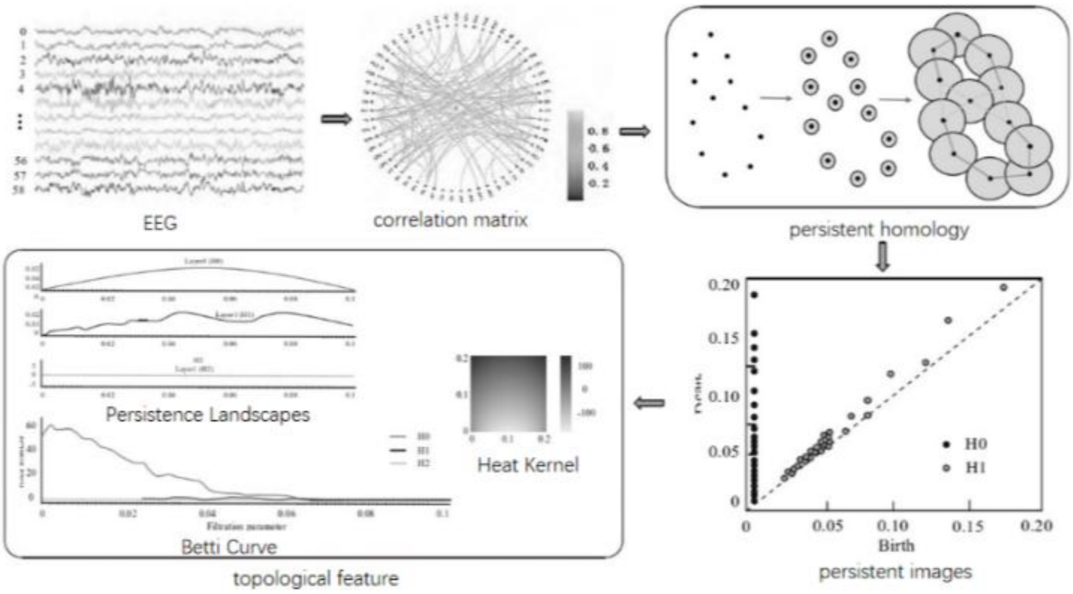

Figure 6. Flowchart of topological feature extraction

Table 2. Topological feature parameter selection

topological feature	Parameter selection
persistent landscape	2-layer 1-parameter
	2-layer 2-parameter
	1-layer 1-parameter
	1-layer 2-parameter
Betti curve	1-parameter
	2-parameter
heat core	Gaussian kernel standard deviation 1.6 1 Fan number
	Gaussian kernel standard deviation 3.2 1 Fan number
	Gaussian kernel standard deviation 1.6 2 Fan number
	Gaussian kernel standard deviation 3.2 2 Fan number
persistent entropy	no

4. Experimental Results and Analysis

4.1. Significant Brain Region Differences

For the data of the subjects in the experiment, the following experimental steps were carried out for each group of subjects separately. Calculate the multilayer overlap degree, multilayer participation coefficient, and multilayer entropy of each node, and average the multilayer entropy values taken in all brain regions to get the overall multilayer entropy of the multilayer brain network of the subject. Based on the constructed multilayer brain network, the coordinates of the point clouds of the same nodes were interchanged, and their persistence graphs were extracted through persistent homology and transformed to obtain the higher-order features of each subject. After that, the network features were analyzed holistically from the perspective of the whole brain.

Independent samples t-test was used to test the differences between the groups, and the results are shown in Figure 7, in which there is a significant difference between the two groups of subjects in the multilayer degree of entropy index, and the multilayer degree of entropy of normal people is significantly higher than that of the patients with schizophrenia scores ($p<0.01$).

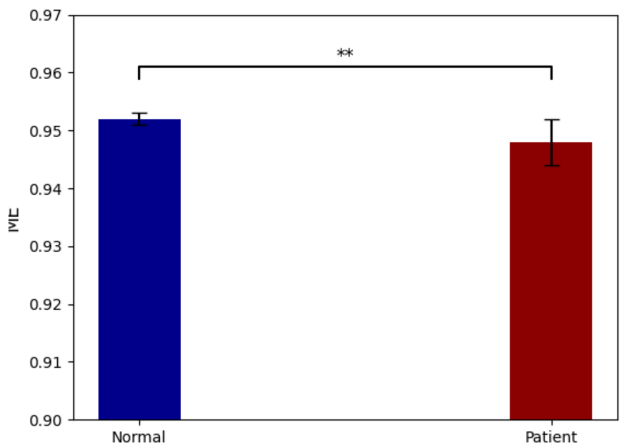

Figure 7. Comparison of EMD between normal and spermatozoa patients

The persistent homology of the two groups of subjects obtained by continuous homology is shown in Figure 8. From the figure, there is significant variability in the persistence maps under the two groups of subjects. The two-dimensional topology of the healthy subjects is more clustered in the higher threshold part of the distribution than that of the seminal patients, indicating that the topology of the healthy subjects still maintains strong connectivity and stability at high thresholds. The topology of the spermatic patients, on the other hand, was more dispersed, indicating that the topology of the spermatic patients showed more variation or instability at lower thresholds.

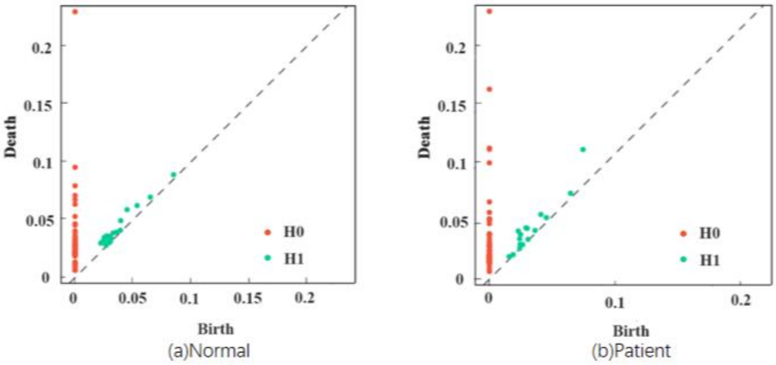

Figure 8. Comparison of normal and patient persistence images

The above results show that the overall multilayer degree of entropy of the multilayer brain network shows a decreasing result after lesioning from a normal person to a spermatoglyphic patient, which is in mutual agreement with the results of the persistence plot observation, and responds to the fact that the brain network shows a decreasing result of the global information processing ability and the overall coordination after lesioning.

Relying on the clinical EEG technology operation guidelines were able to extract 59 brain regions from the EEG data to get the electrode position and name of each brain region. In this section is the integration and separation mechanism of the network is studied in each brain region, calculating the multilayer degree entropy of each node to get the changes of the brain region after the lesion, and fusing with the higher-order features to calculate the weight for ranking to get the results as shown in Table 3 below.

Table 3. Table of Significant Differences in Brain Regions Across the Brain

	title	electrode position	weights
Patient	F8	Right Frontal Cortex	0.183
	T7	Left Temporal Lobe	0.182
	O1	Left Occipital Lobe	0.179
	Fz	Frontocentral Cortex	0.178
	P6	Right Parietal Lobe	0.182
	Fp1	Left Frontal Cortex	0.181
	F7	Left Frontal Cortex	0.180
	P4	Right Parietal Lobe	0.179
	F8	Right Frontal Cortex	0.183
	F5	Left Frontal Cortex	0.182
	F4	Right Frontal Cortex	0.183
	FC5	Left Parietal Lobe	0.182
	F7	Left Frontal Cortex	0.187
	T8	Right Parietal Lobe	0.189
Normal	T7	Left Parietal Lobe	0.176
	Fp1	Left Frontal Cortex	0.179
	F3	Left Frontal Cortex	0.178
	T7	Left Temporal Lobe	0.180
	C4	Right Central Region	0.183
	C3	Left Central Region	0.179

The left parietal lobe is a major region of the brain located at the top and side of the brain, in the left cerebral hemisphere. The parietal lobe is one of the four main lobe-like structures of the brain and is responsible for a variety of perceptual, cognitive and motor functions. This region has also been repeatedly found to be abnormal in structural imaging studies of patients with schizophrenia [22].

The frontal-central cortex is a specific area located at the front of the brain, also known as the central frontal cortex. It is the anterior midline region of the cerebral cortex and is located in the center of the frontal lobe. The brain region plays an important role in cognitive, emotional and behavioral regulation. The frontal-central cortex plays a key regulatory role in many cognitive tasks, emotional processing, and social behaviors [23].

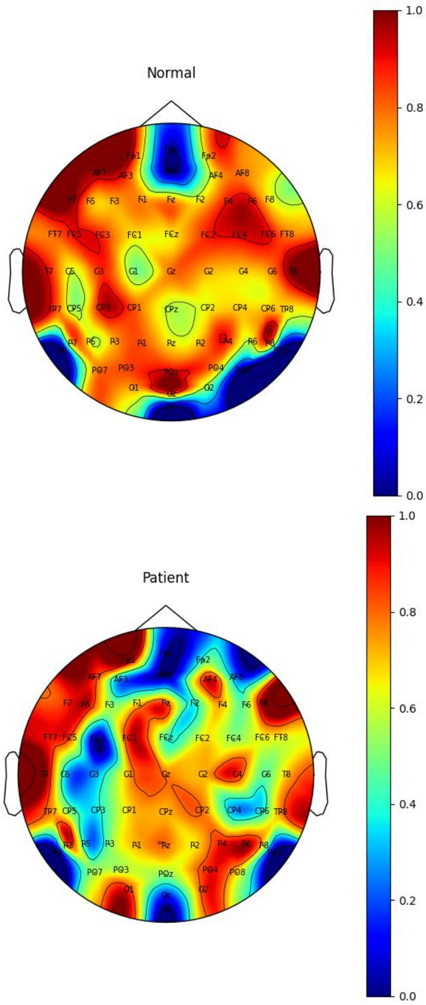

Figure 9. Differences in topography of brain regions between normal and schizophrenia patients

The experimental results showed that the important brain regions were mainly found in the right and left frontal cortex, the left temporal lobe, and the right and left parietal lobes. Specifically: for the right and left frontal cortex, right parietal lobe, and left temporal lobe, the brain regions corresponding to these electrode locations all play important roles in the brain regions of normal people and schizophrenic patients as the main nodes [24]. While for the two electrode positions FC5 and T7 corresponding brain regions play important roles in normal people's brain regions, but the importance decreases after the onset of the disease, in contrast, the importance of the brain regions corresponding to the Fz electrode positions increases, indicating that the frontal-central cortex undergoes important changes after the lesion. These results indicate that the changes in the brain regions of the subjects after the lesion indicate that schizophrenic patients have different degrees of alterations in their perceptual and cognitive functions, and this phenomenon contributes to the further understanding of the pathogenesis of schizophrenia[25]. Brain topography mapping based on the weighted magnitude is shown in Figure 9.

4.2. Classification of Patients with Different Characteristics

Firstly, the four higher-order topological features with multiple entropy extracted from the subjects under each multilayer network were entered into the deep learning and traditional machine learning models (GCN, SVM, CNN, KNN) for classification respectively, and the feature performance was evaluated using the correct rate. Then the traditional higher order features based on each frequency band and multiband fusion to get multilayer network features for machine learning classification model comparison experiments using fivefold cross validation, the results are shown in Table 4. As shown in Table 4 it can be seen that the multimodal persistent features have higher accuracy rate, at the same time, based on the results in Table 4, we use the classifier GCN with the highest accuracy rate to compare the different features with multiple metrics, and under the four metrics of accuracy, precision, recall, and F1 scores, the multimodal persistent features have better performance, and the results are shown in Table 5.

Table 4. Comparison of classification performance of multiple classifiers with different features

Features	GCN	CNN	SVM	KNN
EMD	0.694	0.655	0.643	0.633
PL	0.707	0.693	0.677	0.676
PD	0.716	0.687	0.673	0.644
HK	0.733	0.694	0.684	0.673
PE	0.721	0.701	0.691	0.688
EMD+PL+PD+HK+PE	0.923	0.894	0.889	0.863

From Table 4, it can be seen that multimodal persistent features have higher accuracy rate, also based on the results in Table 4, we use the classifier GCN with the highest accuracy rate to compare different features with multiple indicators, and multimodal persistent features have a better performance under the four indicators of accuracy, precision, recall, and F1 score, and the results are shown in Table 5.

Table 5. GCN model classification performance

Features	Accuracy	Precision	Recall	F1
EMD	0.694	0.714	0.455	0.556
PL	0.707	0.8	0.571	0.667
PD	0.716	0.8	0.615	0.98
HK	0.733	0.894	0.625	0.721
PE	0.721	0.833	0.597	0.694
EMD+PL+PD+ HK+PE	0.923	0.932	0.833	0.880

5. Conclusion

In this study, we propose a multilayer brain network modeling method based on EEG signals for mining changes in brain regions of schizophrenia patients during lesions and classifying them based on the extracted network features. First, we segment the signal into multiple non-overlapping continuous time windows using a determined window length and step size. Then, functional connectivity between single-layer nodes is calculated based on phase-locked values, and a multilayer brain network is constructed. Next, we realize the capture of cross-frequency band information by exchanging the point cloud coordinates of neighboring layers and extract higher-order features by continuous homodyne filtering, and finally realize the extraction of cross-frequency domain information of the multilayer brain network.

The results of the study showed that the best results were obtained using a multilayer network and fusing local and global features for classification. An accuracy of 0.923 was achieved when using a graph convolutional neural network model for classification. this is because the multilayer alarm network-based model with continuous homophony approach is able to capture higher-order topological features across frequency bands that are not accessible to traditional single-layer brain networks. With the constructed multilayer network model and topographic difference maps across frequency bands, we reveal the topological structure and features of EEG data, and revisit the understanding and interpretation of brain functions from the perspective of topology.

Future research can further expand and optimize the multilayer brain network modeling method based on EEG signals. Combining other brain imaging techniques and clinical features to improve the understanding and diagnostic accuracy of psychiatric disorders of the brain and to provide more effective support for individualized treatment and rehabilitation.

References

[1] Buzsáki, G Logothetis, N Singer, W. Scaling brain size, keeping timing: evolutionary preservation of brain rhythms. Neuron, 2013, 80(3): 751-764.

[2] Xing, X-X. Globally aging cortical spontaneous activity revealed by multiple metrics and frequency bands using resting-state functional MRI. Frontiers in Aging Neuroscience, 2021, 13803436.

[3] Lynall, M-E Bassett, D S Kerwin, R, et al. Functional connectivity and brain networks in schizophrenia. Journal of Neuroscience, 2010, 30(28): 9477-9487.

[4] Fan, F Tan, S Huang, J, et al. Functional disconnection between subsystems of the default mode network in schizophrenia. Psychological medicine, 2022, 52(12): 2270-2280.

[5] Battiston, F Nicosia, V Latora, V. Structural measures for multiplex networks. Phys. Rev. E, 2014, 89(3): 032804.

[6] D'Andrea, A Chella, F Marshall, T R, et al. Alpha and alpha-beta phase synchronization mediate the recruitment of the visuospatial attention network through the Superior Longitudinal Fasciculus. NeuroImage, 2019, 188722-732.

[7] Yin, G Chang, Y Zhao, Y, et al. Automatic recognition of schizophrenia from brain-network features using graph convolutional neural network. Asian Journal of Psychiatry, 2023, 87103687.

[8] Tandon, R Nasrallah, H Akbarian, S, et al. The schizophrenia syndrome, circa 2024: What we know and how that informs its nature. Schizophrenia research, 2024, 2641-28.

[9] Xu, F Zhang, J Jin, M, et al. Chimera states and synchronization behavior in multilayer memristive neural networks. Nonlinear dynamics, 2018, 94(2): 775-783.

[10] Ke, M Wang, C Liu, G. Multilayer brain network modeling and dynamic analysis of juvenile myoclonic epilepsy. Frontiers in Behavioral Neuroscience, 2023, 171123534.

[11] Kim, J Lee, D A Lee, H J, et al. Multilayer network changes in patients with migraine. Brain and Behavior, 2023, 13(12): e3316.

[12] Micheloyannis, S Pachou, E Stam, C J, et al. Small-world networks and disturbed functional connectivity in schizophrenia. Schizophrenia research, 2006, 87(1-3): 60-66.

[13] Kindelan, R Frías, J Cerda, M, et al. A topological data analysis based classifier. Advances in Data Analysis and Classification, 2023, 1-46.

[14] Taiwo, F M Islambekov, U Akcora, C G. Explaining the Power of Topological Data Analysis in Graph Machine Learning. arXiv preprint arXiv:2401.04250, 2024.

[15] Wang, Y Ombao, H Chung, M K. Statistical persistent homology of brain signals. In Proceedings of the ICASSP 2019-2019 IEEE International Conference on Acoustics, Speech and Signal Processing (ICASSP), 2019; pp. 1125-1129.

[16] Yip, J H Biagetti, M Cole, A, et al. Cosmology with persistent homology: a Fisher forecast. Journal of Cosmology and Astroparticle Physics, 2024, 2024(09): 034.

[17] Peng, Y Wang, H Sonka, M, et al. PHG-Net: Persistent homology guided medical image classification. In Proceedings of the Proceedings of the IEEE/CVF Winter Conference on Applications of Computer Vision, 2024; pp. 7583-7592.

[18] Yu, B Xie, H Xu, Z. PN-GCN: Positive-negative graph convolution neural network in information system to classification. Information Sciences, 2023, 632411-423.

[19] Kong, H Lou, X Li, Z. Emotional EEG recognition and classification based on GCN combined with LSTM. In Proceedings of the 2024 IEEE International Conference on Medical Artificial Intelligence (MedAI), 2024; pp. 294-301.

[20] Zhang, Y Zhang, Y Yan, D, et al. NIE-GCN: Neighbor Item Embedding-Aware Graph Convolutional Network for Recommendation. IEEE Transactions on Systems, Man, and Cybernetics: Systems, 2024.

[21] Liang, J Wang, Z Han, J, et al. EEG-based driving intuition and collision anticipation using joint temporal-frequency multi-layer dynamic brain network. Frontiers in Neuroscience, 2024, 181421010.

[22] Cao, H Wei, X Zhang, W, et al. Cerebellar functional dysconnectivity in drug-naïve patients with first-episode schizophrenia. Schizophrenia bulletin, 2023, 49(2): 417-427.

[23] Yu, X-M Qiu, L-L Huang, H-X, et al. Comparison of resting-state spontaneous brain activity between treatment-naive schizophrenia and obsessive-compulsive disorder. BMC psychiatry, 2021, 211-14.

[24] Howes, O D Cummings, C Chapman, G E, et al. Neuroimaging in schizophrenia: an overview of findings and their implications for synaptic changes. Neuropsychopharmacology, 2023, 48(1): 151-167.

[25] Chatterjee, I Hilal, B. Investigating the association between symptoms and functional activity in brain regions in schizophrenia: A cross-sectional fmri-based neuroimaging study. Psychiatry Research: Neuroimaging, 2024, 344111870.